Quantum Rabi Oscillation of Trapped Ion Driven by Coherent Pulse Streams

Li Yang,[1] Biyao Yang,[1] and Yufu Chen[2]

[1]*State Key Laboratory of Information Security, Graduate University of Chinese Academy of Sciences, Beijing 100049, China*

[2]*College of Mathematical Science, Graduate University of Chinese Academy of Sciences, Beijing 100049, China*

Abstract

Quantum Rabi oscillations driven by a pulse stream are basic operations in Cirac-Zoller scheme of quantum computation. We investigate the failure probability and population inversion of quantum Rabi oscillation of trapped ion in this case. It is shown that when the wavelength of the driven field is of the order 10^{-6} m, the mean number of photons cannot be greater than 10^4, and the failure probability of quantum Rabi oscillation is of the order 10^{-2} after about 100 coherent 2π pulses considering of the sideband transition in Cirac-Zoller scheme. We find also that the envelope of population inversion is different from the Gaussian function which is that for oscillation driven by a continuous-wave field. The conclusion we arrived at is that the quantum computations via Cirac-Zoller scheme cannot be reliable if the number of Controlled-NOT operation on any physical qubit involved is greater than 100, except making use of driving fields with much smaller wavelength. This conclusion may be independent of any possible technical improvement in future.

I. INTRODUCTION

The quantum Rabi oscillation and the accompanied collapse and revival phenomenon are essential in quantum optics. When a coherent field is used to drive Rabi oscillation, different number state components of the driving field lead to different oscillation amplitudes, and the different amplitudes become uncorrelated gradually. It has been proved that the cosine oscillations are terminated by Gaussian envelope [1].

J. H. Eberly et al. studied the dynamics of coherent Jaynes-Cummings model, in which the field mode is initially a coherent state, and confirmed the existence of periodic spontaneous collapse and revival of coherence [2]. Then, N. B. Narozhny et al. gave a description of the temporal behavior of the dynamic elements of coherent Jaynes-Cummings model [3]. P. L. Knight and P. W. Milonni studied the effects of intense coherent resonant radiation on the dynamics of atoms, and found that Rabi oscillations of state probability amplitudes lead to many new effects in optical spectra [4]. Later, P. L. Knight and P. M. Radmore investigated the coherent Jaynes-Cummings model in a transformed representation emphasizing quantum corrections to the semiclassical Rabi problem, and gave an intuitive explanation of the collapse and revivals of oscillations in the population inversion [5]. H. I. Yoo and J. H. Eberly presented a dynamical theory of an atom with two or three levels interacting with quantized cavity fields in the framework of models of the Jaynes-Cummings type, and discussed phenomena like quantum wave packet collapse and revival [6].

However, quantum Rabi oscillation driven by coherent pulse streams has not been fully investigated. In this paper we discuss it in details. The discussion focus on oscillation of trapped ion, which is a fundamental issue in physics, and has wide applications, such as in Cirac-Zoller physical realization scheme of quantum computations, laser control of chemical reaction [7], etc..

Quantum computers (QC) can solve some problems intractable on classical computers [8], and challenge most public-key cryptosystems currently in use [9, 10]. Many proposals for implementing QC have been raised. The cold ion trap method [11] is a classic one. In this scheme, implementation of quantum logic gates is realized right through the ions' Rabi oscillation driven by pulse streams of laser fields.

C. Monroe et al. [12]demonstrated the essence of controlled-NOT (CNOT) gate in Cirac-Zoller scheme in 1995. The complete CNOT gate was implemented by F. Schmidt-Kaler et al. [13]. Since then, much effort has been made towards large-scale, robust ion trap QC. There is a scheme to perform probabilistic quantum gates on remote trapped atom qubits [14]. A method to achieve scalable quantum computation based on fast quantum gates on an array of trapped ions was also proposed [15]. An experimentally feasible scheme to achieve quantum computation based solely on geometric manipulations of a quantum system [16] offers a possible method for robust quantum computation. In 2009, D. R. Leibrandt et al. [17] developed a scalable, multiplexed chip for ion trap quantum information processing and tested ion lifetimes and heating rate of it.

This paper is arranged as follows: in Section II, we develop a method to describe quantum Rabi transformation of trapped ion after one coherent pulse. In Section III we deal with the relationship between the density matrices for the ion before and after one coherent pulse, and gives failure probability of quantum Rabi oscillation of trapped ion driven by coherent pulse streams. In Section IV we give out some discussions. In Section V some conclusions are reached.

II. QUANTUM RABI TRANSFORMATION OF TRAPPED ION RELATED WITH ONE COHERENT PULSE

A. Modeling

Consider of a two-level ion trapped in a Paul trap interacts with a laser field. The laser field is actually a multimode field, but when the bandwidth of the laser satisfies some requirements, it is justified to take the field to be a single-mode coherent state [18]. Then the ion-field system can be described by Jaynes-Cummings interaction [19]

$$H = \hbar g(e^{-i\phi}\sigma_+ a + e^{i\phi}a^\dagger\sigma_-), \tag{1}$$

where g is the coupling constant, ϕ is the beam phase, σ_+ and σ_- are the raising and lowering operators of the ion, and $a^\dagger$ and a are the creation and annihilation operators of photons respectively. Then the unitary time-evolution operation is given by

$$\begin{aligned} U(t) =& \cos(gt\sqrt{a^\dagger a+1})|1\rangle\langle 1| + \cos(gt\sqrt{a^\dagger a})|0\rangle\langle 0| \\ &- i[e^{i\phi}\frac{\sin(gt\sqrt{a^\dagger a+1})}{\sqrt{a^\dagger a+1}}a|1\rangle\langle 0| + e^{-i\phi}a^\dagger\frac{\sin(gt\sqrt{a^\dagger a+1})}{\sqrt{a^\dagger a+1}}|0\rangle\langle 1|], \end{aligned} \tag{2}$$

here, $|0\rangle$ and $|1\rangle$ denote the ground and excited state of the ion respectively.

The coherent state is usually described by $\sum_{n=0}^{\infty} c_n|n\rangle$, here $|c_n|^2 = \frac{e^{-\bar{n}}\bar{n}^n}{n!}$ is the probability that the state is in the n-photon state. If the ion is initially in the ground state, then the ion-field state is $\sum_{n=0}^{\infty} c_n|0,n\rangle$, the state for the ion-field system at time t is therefore

$$|\Psi(t)\rangle = \sum_{n=0}^{\infty} c_n[\cos(gt\sqrt{n+1})|1,n\rangle - ie^{-i\phi}\sin(gt\sqrt{n+1})|0,n+1\rangle]. \tag{3}$$

Similarly, if the ion is initially in the excited state, then the ion-field state is $\sum_{n=0}^{\infty} c_n|1,n\rangle$, the state for the ion-field system at time t is

$$|\Psi(t)\rangle = \sum_{n=0}^{\infty} c_n[\cos(gt\sqrt{n})|0,n\rangle - ie^{i\phi}\sin(gt\sqrt{n})|1,n-1\rangle]. \tag{4}$$

Now move to the practical case, the ion's initial state is generally a superposition of the ground and excited states, thus initially the ion-field state is $|\psi(0)\rangle = \sum_{n=0}^{\infty} c_n|n\rangle(\alpha|0\rangle + \beta|1\rangle)$, where $|\alpha|^2 + |\beta|^2 = 1$. A single qubit gate is usually implemented through a $k\pi$ pulse, whose duration t_0 satisfy $gt_0\sqrt{\bar{n}} = \frac{k\pi}{2}$, here $\bar{n}$ is the mean number of photons in the pulse. Without loss of generality, consider the case we apply a 2π pulse, then the ion-field state becomes

$$\begin{aligned} |\psi(t)\rangle =& \alpha\{\sum_{n=0}^{\infty} c_n[\cos(\frac{\pi\sqrt{n+1}}{\sqrt{\bar{n}}})|1,n\rangle - ie^{-i\phi}\sin(\frac{\pi\sqrt{n+1}}{\sqrt{\bar{n}}})|0,n+1\rangle\} \\ &+ \beta\{\sum_{n=0}^{\infty} c_n[\cos(\frac{\pi\sqrt{n}}{\sqrt{\bar{n}}})|0,n\rangle - ie^{i\phi}\sin(\frac{\pi\sqrt{n}}{\sqrt{\bar{n}}})|1,n-1\rangle\}. \end{aligned} \tag{5}$$

B. Estimation of mean number of photons

In the discussions followed we need to know the mean number of photons. When a laser beam is applied to a trapped ion, it is actually a scattering problem. The effective interaction area is the same order of magnitude as the scattering cross section. The total resonant scattering cross section for an atomic dipole transition is $\sigma = 3\lambda^2/2\pi$ [20], and for inelastic scattering which we are interested in, the cross section is virtually that for scattering out of the paraxial modes $\sigma_{eff} = 3\lambda^2/8\pi$ [21]. Thus it is the number of photons $\bar{n} = \frac{I\sigma_{eff}t}{\hbar\omega}$ in volume $\sigma_{eff}ct$ that is important for the decoherence of the ion, not $\bar{n'} = \frac{IAt}{\hbar\omega}$ in volume Act, here I is intensity of the laser, t the duration of the laser pulse, and A the cross section area of the beam. The beam can not be focused to less than a wavelength, so we will always have $A > \sigma_{eff}$, thus $\bar{n'} > \bar{n}$ [22].

In estimating the effective mean number of photons of one pulse, we can not apply Jaynes-Cummings model directly. Consider two pulses propagating in opposite directions, then when they meet they form a standing wave. The standing wave fits well into the Jaynes-Cummings model, and the mean number of photons in each pulse is half of that in the standing wave. Thus we only need to focus on mean number of photons in the standing wave. The electric field E can be expressed as

$$E = \mathscr{E}\sqrt{\bar{n}}. \tag{6}$$

$\mathscr{E}$ is usually given as $\mathscr{E} = \sqrt{\frac{\hbar\omega}{\epsilon_0 V}}$[23] , where ω is the frequency of the single mode in a cavity, and V is the volume of the cavity. It can be seen that $V \sim \sigma_{eff}ct$, then $\mathscr{E} = \sqrt{\frac{\hbar}{\epsilon_0\sigma_{eff}\lambda t}}$. Thus

$$\bar{n} = \frac{\epsilon_0\sigma_{eff}ct}{\hbar\omega}E^2. \tag{7}$$

Moreover, for a $k\pi$ pulse, $gt\sqrt{\bar{n}} = \frac{k\pi}{2}$, $g \sim \frac{p\mathscr{E}}{\hbar} = \frac{PE}{\hbar\sqrt{\bar{n}}}$, here $p \sim ea_0$ is the electric dipole moment of the ion, with e the charge of a electron, and a_0 Bohr radius, then we get

$$t = \frac{k\pi\hbar}{2pE}. \tag{8}$$

Then

$$\bar{n} = \frac{k}{4}\frac{\epsilon_0\sigma_{eff}\lambda}{p}E. \tag{9}$$

One case of interest is the sideband transition, where the laser detuning $\Delta = \pm\omega_t$, here ω_t is the frequency of the trap. Sideband transition is necessary for two-qubit gates in quantum computation [11]. For sideband transition, because of AC-Stark shift and off-resonant transitions, the sideband Rabi frequency Ω_+ has upper bound. People have adopted methods to partially cancel the effect, and it seems feasible to have Ω_+ close to ω_t for special temporal and spectral arrangements of the laser field [24, 25].

As we know, $\Omega_+ = \eta\Omega$, so we have

$$\Omega < \frac{\omega_t}{\eta}. \tag{10}$$

here

$$\eta = \frac{2\pi}{\lambda}\sqrt{\frac{\hbar}{2M\omega_t}} \tag{11}$$

is the Lamb-Dicke parameter, with M the mass for a single ion, For Ω, there exists the relation $\Omega = -\frac{ea_0E}{4\hbar}$ [26], then

$$E < \frac{4\hbar\omega_t}{p\eta}. \tag{12}$$

As to ω_t, the separation between ions Δz satisfies [27]

$$\Delta z \sim (\frac{e^2}{4\pi\epsilon_0 M\omega_t^2})^{1/3},$$

so

$$\omega_t \sim \sqrt{\frac{e^2}{4\pi\epsilon_0 M(\Delta z)^3}}. \tag{13}$$

In Eq. (13), Δz should be large enough to ensure individual addressing of ions, thus it can be expressed as $\xi\lambda$, with $\xi \geq 2$, thus ω_t has a corresponding lower limit.

Thus, from Eqs. (11) to (13), we get

$$E < \frac{2\sqrt{2\hbar}}{p\pi}(\frac{e^2}{4\pi\epsilon_0})^{\frac{3}{4}} M^{-\frac{1}{4}}\xi^{-\frac{9}{4}}\lambda^{-\frac{5}{4}}. \tag{14}$$

Substitute E in Eq. (9) with that in Eq. (13), we get

$$\begin{aligned}\bar{n} &< \frac{k}{2}\frac{3\sqrt{2\hbar}\epsilon_0}{8\pi^2 p^2}(\frac{e^2}{4\pi\epsilon_0})^{\frac{3}{4}} M^{-\frac{1}{4}}\xi^{-\frac{9}{4}}\lambda^{\frac{7}{4}} \\ &= \frac{3\epsilon_0^{\frac{1}{4}}}{32a_0^2\pi^{\frac{11}{4}}}\sqrt{\frac{\hbar}{e}}kM^{-\frac{1}{4}}\xi^{-\frac{9}{4}}\lambda^{\frac{7}{4}} \\ &= 6\times 10^7 kM^{-\frac{1}{4}}\xi^{-\frac{9}{4}}\lambda^{\frac{7}{4}}.\end{aligned} \tag{15}$$

In the cases we consider here, $k \leq 2$, $9\text{u} \leq M \leq 200\text{u}$, with $\text{u} = 1.66057\times 10^{-27}$ kg. When $M = 9\text{u}, k = 2, \xi = 2, \lambda \sim 10^{-6}$ m, we get the maximum for mean number of photons when optical frequency is used

$$\bar{n} \sim 2.3\times 10^3.$$

For $\xi = 5$ case which is the best result experimentally reached [28], we can get

$$\bar{n} \sim 2.9\times 10^2.$$

When microwaves are used to drive the oscillation, the frequency ν is usually below 10GHz [25]; and it should be much greater than $1/2\pi$ GHz [27], which is the upper bound for a phonon used in experiments. Suppose $\nu > 5$ GHz, then 3×10^{-2} m $< \lambda < 0.38$ m, then for $\xi = 5$ case, we get

$$2.9\times 10^9 < \bar{n} < 1.7\times 10^{12}.$$

There exists another way to calculate the mean number of photons in a $k\pi$ pulse [18]: they considered the situation where a single laser is used to drive Rabi oscillation of the atom, and adopted the formalism introduced by K. J. Blow et al. [29], taking the laser as a continuous-mode coherent state, then they worked out the interaction time t for $k\pi$ pulse is

$$t = \frac{k\pi\hbar}{d}\sqrt{\frac{\epsilon_0 cA}{2P}}, \tag{16}$$

here d is the coupling distant between the atom and laser, and for a dipole transition it is the atomic dipole moment p, and W is the power of the laser. Thus, the mean number of photons in one $k\pi$ pulse is

$$\bar{n} \approx \frac{Pt}{\hbar\omega_L} = \frac{k\pi}{\omega_L d}\sqrt{\frac{\epsilon_0 cAP}{2}}, \tag{17}$$

where ω_L is the frequency of the fictitious single-mode coherent state. Thus, obviously, they take all the photons in area A as effective photons when considering the interaction, but actually the effective photons is much less.Substitute parameters in Eq. (17) with that in our approach, and use $A > 2\mu\text{m} \times 2\mu\text{m}$ [28], the mean number of photons with $\lambda \sim 10^{-6}$ m is 1.4×10^4 when $\xi = 5$.

C. The Density Matrix

The corresponding density matrix for the state in Eq. (5) is $\rho^{(1)}_{total} = |\psi(t)\rangle\langle\psi(t)|$. This matrix contains the information of both the ion and the field, but we are interested only in the ion. Thus we perform a partial trace over the field to obtain the reduced state of the ion alone, the reduced density matrix $\rho^{(1)}$ is

$$\rho^{(1)} = \begin{pmatrix} |\alpha|^2 s_4 + i(\alpha\beta^* - \alpha^*\beta)s_2 + |\beta|^2(1-s_6) & \alpha\beta^* s_5 + i(|\alpha|^2 s_1 - |\beta|^2 s_7) + \alpha^*\beta s_3 \\ \alpha^*\beta s_5 - i(|\alpha|^2 s_1 + |\beta|^2 s_7) + \alpha\beta^* s_3 & |\alpha|^2(1-s_4) - i(\alpha\beta^* - \alpha^*\beta)s_2 + |\beta|^2 s_6 \end{pmatrix},$$

$$
\begin{aligned}
s_1 &= \sum_{n=0}^{\infty} \frac{\mathrm{e}^{-\bar{n}}\bar{n}^n}{n!}\sqrt{\frac{\bar{n}}{n+1}}\cos(\frac{\pi\sqrt{n}}{\sqrt{\bar{n}}})\sin(\frac{\pi\sqrt{n+1}}{\sqrt{\bar{n}}}),\\
s_2 &= \sum_{n=0}^{\infty} \frac{\mathrm{e}^{-\bar{n}}\bar{n}^n}{n!}\sqrt{\frac{\bar{n}}{n+1}}\sin(\frac{2\pi\sqrt{n+1}}{\sqrt{\bar{n}}}),\\
s_3 &= \sum_{n=0}^{\infty} \frac{\mathrm{e}^{-\bar{n}}\bar{n}^n}{n!}\sqrt{\frac{n}{n+1}}\sin(\frac{\pi\sqrt{n}}{\sqrt{\bar{n}}})\sin(\frac{\pi\sqrt{n+1}}{\sqrt{\bar{n}}}),\\
s_4 &= \sum_{n=0}^{\infty} \frac{\mathrm{e}^{-\bar{n}}\bar{n}^n}{n!}\cos(\frac{\pi\sqrt{n}}{\sqrt{\bar{n}}})^2,\\
s_5 &= \sum_{n=0}^{\infty} \frac{\mathrm{e}^{-\bar{n}}\bar{n}^n}{n!}\cos(\frac{\pi\sqrt{n}}{\sqrt{\bar{n}}})\cos(\frac{\pi\sqrt{n+1}}{\sqrt{\bar{n}}}),\\
s_6 &= \sum_{n=0}^{\infty} \frac{\mathrm{e}^{-\bar{n}}\bar{n}^n}{n!}\cos(\frac{\pi\sqrt{n+1}}{\sqrt{\bar{n}}})^2,\\
s_7 &= \sum_{n=0}^{\infty} \frac{\mathrm{e}^{-\bar{n}}\bar{n}^n}{n!}\sqrt{\frac{n}{\bar{n}}}\cos(\frac{\pi\sqrt{n+1}}{\sqrt{\bar{n}}})\sin(\frac{\pi\sqrt{n}}{\sqrt{\bar{n}}}).
\end{aligned}
\tag{18}
$$

D. Calculation of the sums in the density matrix

We can't get accurate results for s_1 to s_7 in $\rho^{(1)}$ via usual method. The precision of method generally used is of the order $\frac{1}{\sqrt{\bar{n}}}$, which is not enough to validate the result for the iteration. Our approach with much better precision is as follows.

1. *The approach*

Given one of the sums in $\rho^{(1)}$ mentioned above, for example,

$$s_1(\bar{n}) = \sum_{n=0}^{\infty} \frac{\mathrm{e}^{-\bar{n}}\bar{n}^n}{n!}\sqrt{\frac{\bar{n}}{n+1}}\cos(\frac{\pi\sqrt{n}}{\sqrt{\bar{n}}})\sin(\frac{\pi\sqrt{n+1}}{\sqrt{\bar{n}}}),$$

here we assume $\bar{n} = 10^4$.

1. First deal with the part

$$f_0(n,\bar{n}) = \sqrt{\frac{\bar{n}}{n+1}}\cos(\frac{\pi\sqrt{n}}{\sqrt{\bar{n}}})\sin(\frac{\pi\sqrt{n+1}}{\sqrt{\bar{n}}}),$$

substitute n in $f_0(n,\bar{n})$ with $(x+1)\bar{n}$, we get

$$f_1(x,\bar{n}) = \sqrt{\frac{\bar{n}}{1+\bar{n}(1+x)}}\cos\left(\frac{\pi\sqrt{\bar{n}(1+x)}}{\sqrt{\bar{n}}}\right)\sin\left(\frac{\pi\sqrt{1+\bar{n}(1+x)}}{\sqrt{\bar{n}}}\right).$$

This actually rewrites $f_0(n, \bar{n})$ as a function of $x = \frac{n-\bar{n}}{\bar{n}}$ and $\bar{n}$, and $x < 1$ is satisfied for $n < 2\bar{n}$.

2. Do Taylor expansion for$f_1(x, \bar{n})$at $x = 0$, to ensure a sufficiently high precision, we expand it to x^{10}, and we get $f_2(x, \bar{n})$.

3. Sums like $\sum_{n=0}^{\infty} \frac{\mathrm{e}^{-\bar{n}}\bar{n}^n}{n!} n^k$ can get accurate results, so we replace x in $f_2(x, \bar{n})$ by $\frac{n-\bar{n}}{\bar{n}}$, and use $\bar{n} = 10^6$. Then we get $f_3(n)$.

4. Use $f_3(n)$ instead of $f_0(n, \bar{n})$ in the expression of $s_0(\bar{n})$ and calculate the new sum. The result is $f_4(\bar{n})$.

5. Again use $\bar{n} = 10^4$, and we obtain a high-precision result of the original sum. The value for s_1 to s_7 in the cases where we expand $f_1(x, \bar{n})$ to x^{10} and x^{15} are shown in Table I.

TABLE I: Values for s_1 to s_7, here $\bar{n} = 10^4$. Value1 denote value of the sums when we expand x to x^{10} and Value2 denote that when we expand x to x^{15}. Value1 and Value2 are same to a precision of 10^{-23}.

Sum	Value1	Value2
s_1	0.000039303916656063668561519091	0.000039303916656063668561194770
s_2	0.000039265164255300772996074590	0.000039265164255300772995750283
s_3	0.000246659192761352167541307293	0.000246659192761352167542402758
s_4	0.999753309972685637856777333369	0.999753309972685637856776237858
s_5	0.999753316133881571308212070145	0.999753316133881571308210974684
s_6	0.999753322301165250291025614276	0.999753322301165250291024518866
s_7	0.000039226416698193975826600887	0.000039226416698193975830095264

2. The precision of our approach

(1) For a given integer l, there exists a appropriate integer k, such that

$$\sum_{n=0}^{k} e^{-\bar{n}} \frac{\bar{n}^n}{n!} < \frac{1}{\bar{n}^l}. \tag{19}$$

Proof. For each i satisfying $i \leq k+1 < \bar{n}$, we have $\frac{\bar{n}^i}{i!} < \frac{\bar{n}^{k+1}}{(k+1)!}$, thus we can get

$\sum_{n=0}^{k} \frac{\bar{n}^n}{n!} < (k+1)\frac{\bar{n}^{k+1}}{(k+1)!} = \frac{\bar{n}^{k+1}}{k!}$, so the sufficient condition for (19) is $\frac{\bar{n}^{k+1}}{k!} < \frac{e^{\bar{n}}}{\bar{n}^l}$, i.e.

$$\frac{\bar{n}^{k+l+1}}{k!} < e^{\bar{n}}. \tag{20}$$

From Stirling's formula

$$k! = \sqrt{2\pi k}(\frac{k}{e})^k e^{\frac{\theta}{12k}}, 0 < \theta < 1, \tag{21}$$

then (20) becomes

$$\frac{1}{\sqrt{2\pi k}}(\frac{e}{k})^k e^{-\frac{\theta}{12k}}\bar{n}^{k+l+1} < e^{\bar{n}}, \tag{22}$$

and the sufficient condition for (22) is $(\frac{e}{k})^k\bar{n}^{k+l+1} < e^{\bar{n}}$.

Denote $k = \bar{n} - \alpha\sqrt{\bar{n}}$, we then have

$$\frac{\bar{n}^{\bar{n}-\alpha\sqrt{\bar{n}}+l+1}e^{\bar{n}-\alpha\sqrt{\bar{n}}}}{(\bar{n}-\alpha\sqrt{\bar{n}})^{\bar{n}-\alpha\sqrt{\bar{n}}}} < e^{\bar{n}},$$

i.e.

$$\frac{\bar{n}^{l+1}}{(1-\frac{\alpha}{\sqrt{\bar{n}}})^{\frac{\sqrt{\bar{n}}}{\alpha}(\alpha\sqrt{\bar{n}}-\alpha^2)}} < e^{\alpha\sqrt{\bar{n}}}. \tag{23}$$

When $\alpha << \sqrt{\bar{n}}$, (23) equals $\frac{\bar{n}^{l+1}}{(\frac{1}{e})^{\alpha\sqrt{\bar{n}}-\alpha^2}} < e^{\alpha\sqrt{\bar{n}}}$, i.e. $\alpha^2 > (l+1)\ln\bar{n}$. Then the sufficient condition for (19) is

$$\sqrt{\bar{n}} >> \alpha > \sqrt{(l+1)\ln\bar{n}}, \tag{24}$$

which equals to $k < \bar{n} - \sqrt{(l+1)\bar{n}\ln\bar{n}}$.

(2) For a given integer l, there exists a appropriate integer k, such that

$$\sum_{n=k}^{\infty} e^{-\bar{n}}\frac{\bar{n}^n}{n!} < \frac{1}{\bar{n}^l}. \tag{25}$$

Proof.

$$\sum_{n=k}^{n} e^{-\bar{n}}\frac{\bar{n}^n}{n!} = e^{-\bar{n}}\frac{\bar{n}^k}{k!}\sum_{n=k}^{\infty}\frac{\bar{n}^{n-k}k!}{n!} = e^{-\bar{n}}\frac{\bar{n}^k}{k!}\sum_{n=k}^{\infty}\frac{\bar{n}^{n-k}}{n(n-1)\cdots(k+1)}$$
$$< e^{-\bar{n}}\frac{\bar{n}^k}{k!}\sum_{n=k}^{\infty}(\frac{\bar{n}}{k+1})^{n-k} = e^{-\bar{n}}\frac{\bar{n}^k}{k!}\frac{k+1}{k+1-\bar{n}}.$$

Let $\frac{k+1}{k+1-\bar{n}} < k$, that means

$$k > \bar{n} + \frac{1}{\bar{n}}. \tag{26}$$

Suppose (26) is fulfilled, we get a sufficient condition for (25):

$$e^{-\bar{n}}\frac{\bar{n}^{k-1}}{(k-1)!} < \frac{1}{\bar{n}^{l+1}},$$

then from Stirling's formula we get the sufficient condition for (25):

$$(\frac{\bar{n}e}{k-1})^{k-1} < \frac{e^{\bar{n}}}{\bar{n}^{l+1}}. \tag{27}$$

Let $\lambda = \frac{\bar{n}}{k-1} < 1$, here we require $k-1 > \bar{n}$, i.e.

$$k > \bar{n} + 1. \tag{28}$$

It can be seen that (28) implies (26). When (28) is fulfilled, a sufficient condition for (25) is

$$(\frac{e}{\eta})^{\lambda} - e\lambda > 0, \tag{29}$$

where $\eta = (\sqrt[\bar{n}]{\bar{n}})^{l+1}$.

Define

$$f(x) = (\frac{e}{\eta})^{x} - ex,$$

then solving (25) can be reduced to finding zero point of $f(x)$. Suppose $f(x_0) = 0$, then it is demanded that $\lambda < x_0$, i.e.

$$k > \frac{\bar{n}}{x_0} + 1, \tag{30}$$

which is a solution of (25). We can have

$$\eta = (\sqrt[\bar{n}]{\bar{n}})^{l+1} = e^{\frac{l+1}{\bar{n}}\ln\bar{n}} \approx 1 + (l+1)\frac{\ln\bar{n}}{\bar{n}} \overset{\triangle}{=} 1 + \delta,$$

here $\delta << 1$. From $f(x_0) = 0$, we get $x_0(1 - \ln\eta) = 1 + \ln x_0$, it can be seen that $x_0 < 1$. Let $x_0 = 1 - \Delta$, from $\ln(1+x) \approx x - \frac{1}{2}x^2$, we get

$$\Delta \approx \sqrt{2}\sqrt{\delta} - \delta + \frac{1}{2\sqrt{2}}\delta\sqrt{\delta} + \cdots$$

$$\frac{1}{x_0} \approx 1 + \Delta \approx 1 + \sqrt{2}\sqrt{\delta} = 1 + \sqrt{2(l+1)\frac{\ln\bar{n}}{\sqrt{\bar{n}}}}.$$

Therefore

$$k = \bar{n} + \alpha\frac{\sqrt{\ln\bar{n}}}{\sqrt{\bar{n}}}.$$

For $\bar{n} = 10^4$, if the precision demanded is 10^{-20}, then $l = 5$,

$$k = \bar{n} + 4\sqrt{3}\frac{\sqrt{\ln 10}}{\sqrt{\bar{n}}} = \bar{n} + \frac{10.513}{\sqrt{\bar{n}}}.$$

For $\bar{n} = 10^6$, if the precision demanded is 10^{-20}, then $l = 3.3$,

$$k = \bar{n} + \frac{10.900}{\sqrt{\bar{n}}}.$$

We expand $f_1(x, \bar{n})$ at $x = 0$ to x^{15}, and find the value for the sum is the same to a precision of 10^{-23} with that when we expand $f_1(x, \bar{n})$ to x^{10} (see Table I). The possible reason may be that in the proof above, we didn't take into account the periodicity of trigonometric functions. The precision of the sum's value can be remarkably improved since the positive and negative values would cancel. Thus the precision is probably smaller than 10^{-23}.

III. FAILURE PROBABILITY OF THE QUANTUM RABI OSCILLATION OF TRAPPED ION DRIVEN BY COHERENT PULSE STREAMS

A. Relationship between the density matrices for the ion before and after one coherent pulse

The final state $\rho^{(1)}$ in Eq. (18) describes the state of the ion after one 2π pulse when $\bar{n} = 10^4$, and the density matrix of corresponding initial state is

$$\rho^{(0)} = \begin{pmatrix} |\alpha|^2 & \alpha\beta^* \\ \alpha^*\beta & |\beta|^2 \end{pmatrix}. \tag{31}$$

Now we consider the relationship between $\rho^{(1)}$ and $\rho^{(0)}$, so as to get the state of the ion after a stream of coherent pulses. For a single ion, the density matrix ρ satisfies the condition $\rho = \frac{1}{2}(I + \vec{r} \cdot \vec{\sigma})$ [30], $\vec{r} = (r_x, r_y, r_z)$, known as the Bloch vector for state ρ, is a real three-dimensional vector such that $|\vec{r}| \leq 1$, $\vec{\sigma}$ denote the vector of Pauli matrices.

Let $\vec{r}^{(i)} = (r_x^{(i)}, r_y^{(i)}, r_z^{(i)})$ denotes the Bloch vector of $\rho^{(i)}$, we can get $\vec{r}^{(0)}$ and $\vec{r}^{(1)}$. Let $\vec{r}^{(1)} = M\vec{r}^{(0)} + \vec{c}$, here M is a 3×3 matrix and $\vec{c}$ a three-dimensional vector, we get

$$M = \begin{pmatrix} s_3 + s_5 & 0 & 0 \\ 0 & s_5 - s_3 & -(s_1 + s_7) \\ 0 & 2s_2 & s_4 + s_6 - 1 \end{pmatrix}, \tag{32}$$

$$\vec{c} = (0, s_7 - s_1, s_4 - s_6), \tag{33}$$

values for $s_i, i = 1, \cdots, 7$ are those shown in Table I.

B. Final state of the ion after a pulse stream

Provided $\vec{r}^{(i)} = M\vec{r}^{(i-1)} + \vec{c}$, then

$$\vec{r}^{(i)} = M^i\vec{r}^{(0)} + (M^{i-1} + \cdots + M + I)\vec{c},$$

the state of the ion after i 2π pulses is

$$\rho^{(i)} = \frac{1}{2}(I + \vec{r}^{(i)} \cdot \vec{\sigma}). \tag{34}$$

C. Envelope of population inversion after coherent pulse streams

Suppose the initial state is $|1\rangle$, if we have applied a $k\pi$ pulse stream, then define

$$W_m \triangleq \frac{1}{2}(1 - r_z^{(m)}) - \frac{1}{2}(1 + r_z^{(m)}) = -r_z^{(m)},$$

where $m = 0, 2/k, 4/k, 6/k, \cdots$. We plot W_m as a function of Rabi period N which is actually the envelope of population inversion in the 2π pulse case when $\bar{n} = 10^4$ in Fig.(1a), and show derivative at the points sampled in Fig.(1b). The result is the envelope of population inversion of oscillations driven by pulse streams is not a Gaussian function, which describes the envelope of inversion for oscillations driven by a continuous-wave (cw) field.

D. Accuracy of gate operation

Suppose we have applied m coherent pulses and reached a state $\rho^{(m)}$. Let $|\Psi\rangle$ be the expected state, then the failure probability of the Rabi oscillation driven by that pulse is

$$p_f = 1 - \langle\Psi|\rho^{(m)}|\Psi\rangle \triangleq 1 - p_s.$$

From Eq. (34) and the relation for pure state

$$\rho^{(i)} = |\alpha_i|^2|0\rangle\langle 0| + \alpha_i\beta_i^*|0\rangle\langle 1| + \beta_i\alpha_i^*|1\rangle\langle 0| + |\beta_i|^2|1\rangle\langle 1|,$$

we can get for 2π pulse stream

$$\begin{aligned} p_s &= (\alpha^*\langle 0| + \beta^*\langle 1|)\rho^{(m)}(\alpha|0\rangle + \beta|1\rangle) \\ &= |\alpha|^2\rho_{11}^{(m)} + |\beta|^2\rho_{22}^{(m)} + \alpha^*\beta\rho_{12}^{(m)} + \alpha\beta^*\rho_{21}^{(m)} \\ &= \frac{1}{2}(1 + r_z^{(0)}r_z^{(m)}1 + r_x^{(0)}r_x^{(m)} + r_y^{(0)}r_y^{(m)}) \\ &= \frac{1}{2}(1 + \vec{r}^{(0)} \cdot \vec{r}^{(m)}), \end{aligned} \tag{35}$$

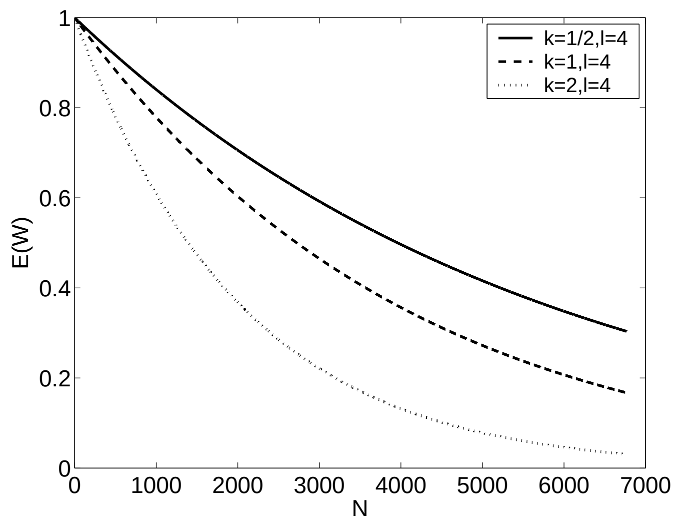

(a) Inversion

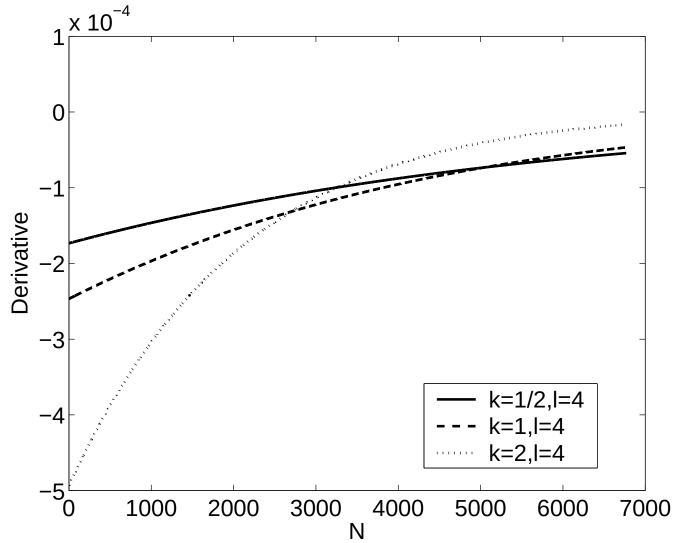

(b) Derivative calculated

FIG. 1: Envelope of population inversion E(W) versus number of Rabi periods N. Here 2π pulses are applied and $\bar{n} = 10^4$. In (a) we plot the envelope of inversion, which looks different from Gaussian functions. In (b) we show derivative of the envelope, and show it is definitely different from that of Gaussian functions.

for a mixed state, $\vec{r} < 1$, then $p_s < 1$.

It can be seen that

$$\vec{r} \cdot \vec{r}^{(m)} = (\vec{r}^{(0)})^T M^m \vec{r}^{(0)}, \tag{36}$$

then

$$p_s = \frac{1}{2}[1 + (\vec{r}^{(0)})^T M^m \vec{r}^{(0)}]$$

The failure probability for different $k\pi$ pulses and mean number of photons are given in Fig. (2). It can be seen that the failure probability increases with the number of Rabi periods, and grows with the value k. Moreover, it is in inverse proportion to mean number of photons $\bar{n}$.

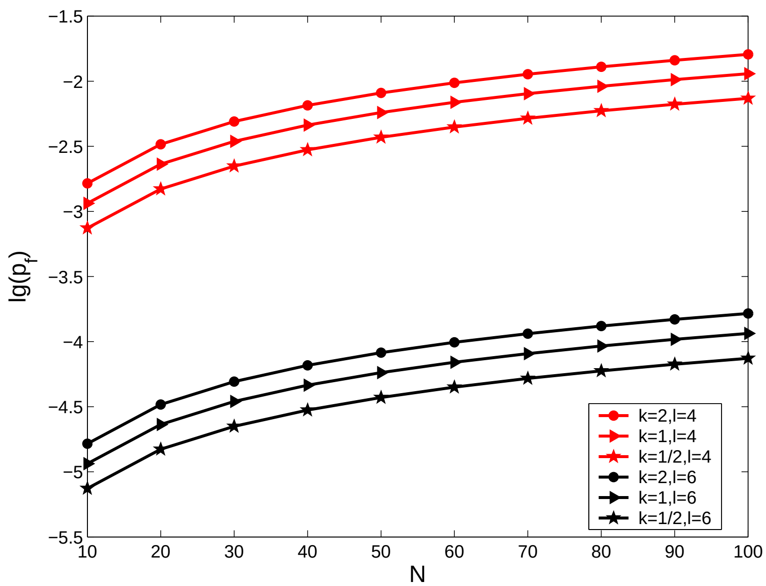

FIG. 2: Logarithm of failure probability lg (p_f) versus number of Rabi periods N. Here $k\pi$ pulses are applied and $\bar{n} = 10^l$. It can be seen that the failure probability increases with the number of Rabi periods and the value k. Moreover, it is in inverse proportion to mean number of photons $\bar{n}$.

The fidelity of $\rho^{(m)}$ and $|\Psi\rangle$ is

$$F(|\Psi\rangle, \rho^{(m)}) = \sqrt{\langle\Psi|\rho_m|\Psi\rangle} = \sqrt{1 - p_f}. \tag{37}$$

We can also get the trace distance between $\rho^{(m)}$ and $|\Psi\rangle$ under 2π pulse stream [30]

$$D(|\Psi\rangle, \rho^{(m)}) = \frac{1}{2}|\vec{r}^{(0)} - \vec{r}^{(m)}|.$$

IV. DISCUSSIONS

A. Threshold theorem of fault-tolerant quantum computation

In ion trap quantum computers, we usually perform many operations on one ion to implement an algorithm. As we have derived, the failure probability of gate operation is of order 10^{-2} after approximate 90 operations.

However, there exists a threshold theorem in quantum computation, which declares that an arbitrarily long quantum computation can be performed reliably if the failure probability of each quantum gate is less than a critical value. One form of this theorem is as follows [30]:

A quantum circuit containing $p(n)$ gates may be simulated with probability of error at most ϵ using

$$O(poly(log(p(n)/\epsilon))p(n)) \tag{38}$$

gates on hardware whose components fail with probability at most p, provided p is below some constant threshold, $p \leq p_{th}$, and given reasonable assumptions about the noise in the underlying hardware.

There has been many discussions about the value of the threshold. M. Liang and L. Yang has pointed out that [31], the optimal error-correction period to get maximum threshold depends on the value of level number of concatenated quantum error-correction code. Knill used numerical calculations and obtained a threshold of the order 10^{-2} [32]. Then, P. Aliferis et al. reached a threshold of 10^{-3} with provable constructions [33]. If the failure probability for a quantum gate is beyond the threshold, then the whole quantum computation will not be reliable. Thus for ion trap quantum computers, after 90 2π sideband operations on one ion, the computation will not be reliable.

B. Error propagation

The error in the calculation is spread as follows: in the beginning to ensure the precision of final result, we calculate the sum s_1 to s_7 with precision (10^{-23}). During further computations, these errors go into M and $\vec{r}$. In the calculation of density matrix $\rho^{(m)}$ after m times of successive operations, the errors from M and $\vec{r}$ spread into $\rho^{(m)}$. Finally, the precision of failure probability and population inversion we get is at least 10^{-8}.

C. An application of our results in quantum computation

Single qubit and CNOT gates are universal for quantum computation. The quantum nature of $k\pi$ pulses first bring about errors in single qubit gates themselves. Moreover, in the implementation of Cirac-Zoller gate in an ion trap [11], they use sideband transitions three times to complete a CNOT gate, including one 2π transition and two π transitions.

As we have calculated, error for the 2π sideband transition is the largest compared to that of π and $\pi/2$, which amounts to 10^{-2} after approximately 90 operations when $\bar{n} = 10^4$. This failure probability is already beyond the well-recognized threshold. Then the total CNOT gate will not be implemented reliably.

Moreover, there also exists a two-qubit gate scheme totally different from the Cirac-Zoller gate [34]. In the scheme implemented by the NIST group [35], they state that off-resonant excitations of the stronger carrier transition is absent, which allows a greater gate speed thus a higher laser intensity. In addition, additional Stark shifts can be efficiently suppressed by choosing almost perpendicular and linear polarizations for the laser beams [36]. Hence, studies on this type of gate may lead to different results.

For Rabi oscillation driven by microwaves, the failure probability may be much smaller because of a large mean number of photons. However, the corresponding qubits manipulated by microwaves are always Zeeman or the hyperfine structures. For the Zeeman structure, a strong field may shift the corresponding levels and change the qubits. Then for the hyperfine structure arisen from nuclear spin, the magnetic moment caused by nuclear spin will possibly have a non-negligible interaction with strong driving fields and also change the qubits. Factors above increase failure probability, then whether the total fidelity could be improved is still an open problem.

V. CONCLUSIONS

Based on the collapse and revival phenomenon of quantum Rabi oscillation driven by a coherent field, and the fact that similar oscillation driven by a pulse stream is a basic operation in Cirac-Zoller scheme of quantum computation, we have derived the failure probability of quantum Rabi oscillation of trapped ion driven by coherent pulse streams instead of a cw field. The failure probability of sideband transition driven by $\pi/2$ pulse stream is the smallest, and in the 2π pulse stream case it is the largest.

Moreover, for Cirac-Zoller gate in ion-trap quantum computers, one sideband transition driven by 2π pulse stream is required to implement the gate. When the wavelength of the driven field is of the order 10^{-6} m and $\bar{n} = 10^4$, the failure probability of quantum Rabi oscillation is of the order 10^{-2}, which is beyond the well-recognized threshold, after 90 coherent 2π pulses considering of the sideband transition in Cirac-Zoller scheme. For Rabi oscillation driven by microwaves, the failure probability may be much smaller because of a large mean number of photons, but other factors arise which increase failure probability, then whether the total fidelity could be improved is still an open problem.

Yang and Chen has pointed out that besides depth of logical operation which describes an algorithm, there also exists a permitted depth of logical operation, which physically limit the number of operations on any physical qubit. If the permitted depth of logical operation is less than the depth of logical operation of an algorithm, then the algorithm will not be implemented reliably [37]. Considering of the result given above and the threshold theorem of fault-tolerant quantum computation, the quantum computations with Cirac-Zoller scheme cannot be still reliable as the depth of logical operation of an algorithm is greater than 90. This limitation may be independent of any possible technical improvement in future.

Besides, for the quantum Rabi oscillation of trapped ion driven by coherent pulse streams, we should note that the envelope of population inversion is different from a standard Gaussian function which is the envelope of oscillation driven by a cw field.

ACKNOWLEDGMENTS

We would like to thank Z. W. Zhou and Y. S. Zhang for useful discussions. This work was supported by the National Natural Science Foundation of China under Grant No. 60573051.

[1] F. W. Cummings, Phys. Rev. **140**, 1051 (1965).

[2] J. H. Eberly, N. B. Narozhny, and J. J. Sanchez-Mondragon, Phys. Rev. Lett. **44**, 1323 (1980).

[3] N. B. Narozhny, J. J. Sanchez-Mondragon, and J. H. Eberly, Phys. Rev. A **23**, 236 (1980).

[4] P. L. Knight and P. W. Milonni, Phys. Rep. **66**, 21 (1980).

[5] P. L. Knight and P. M. Radmore, Phys. Rev. A **26**, 676 (1982).

[6] H. I. Yoo and J. H. Eberly, Phys. Rep. **118**, 239 (1985).

[7] Q. T. Meng, G. H. Yang, and K. L. Han, Int. J. Quantum. Chem. **95**, 30 (2003).

[8] P. W. Shor (IEEE Press, Los Alamitos, 1994).

[9] R. L. Rivest, A. Shamir, and L. Adleman, Comm. ACM **21**, 120 (1978).

[10] W. Diffie and M. Hellman, IEEE Trans. Inf. Theory **22**, 644 (1976).

[11] J. I. Cirac and P. Zoller, Phys. Rev. Lett. **74**, 4091 (1995).

[12] C. Monroe, D. M. Meekhof, B. E. King, W. M. Itano, and D. J. Wineland, Phys. Rev. Lett. **75**, 4714 (1995).

[13] F. Schmidt-Kaler, H. Häffner, M. Riebe, S. Gulde, G. P. T. Lancaster, T. Deuschle, C. Becher, C. F. Roos, J. Eschner, and R. Blatt, Nature **422**, 408 (2003).

[14] L. M. Duan, M. J. Madsen, D. L. Moehring, P. Maunz, R. N. Kohn, and C. Monroe, Phys. Rev. A **73** (2006).

[15] L. M. Duan, Phys. Rev. Lett. **93** (2004).

[16] L. M. Duan, J. I. Cirac, and P. Zoller, Science **292**, 1695 (2001).

[17] D. R. Leibrandt, J. Labaziewicz, R. J. Clark, I. L. Chuang, R. J. Epstein, C. Ospelkaus, J. H. Wesenberg, J. J. Bollinger, D. Leibfried, D. J. Wineland, D. Stick, J. Sterk, C. Monroe, C. S. Pai, Y. Low, R. Frahm, and R. E. Slusher, Quantum Inf. Comput. **9**, 901 (2009).

[18] S. J. Enk and H. J. Kimble, Quantum Inf. Comput. **2**, 1 (2002).

[19] E. T. Jaynes and F. W. Cummings, in *Proceedings of the IEEE*, Vol. 51 (IEEE Press, Los Alamitos, 1963) p. 89.

[20] C. Cohen-Tannoudji, J. Dupont-Roc, and G. Grynberg, *Atom-Photon Interactions* (Wiley, 1992).

[21] A. Siberfarb and I. H. Deutsch, Phys. Rev. A **68**, 013817 (2003).

[22] J. Gea-Banacloche(2002), e-print: quant-ph/0212027.

[23] M. Sargent, M. O. Scully, and W. E. Lamb, *Laser Physics* (Addison-Wesley Pub. Co., 1974).

[24] A. Steane, C. F. Roos, D. Stevens, A. Mundt, D. Leibfried, F. Schmidt-Kaler, and R. Blatt, Phys. Rev. A **62**, 042305 (2000).

[25] H. Häffner, C. F. Roos, and R. Blatt, Phys. Rep. **469**, 155 (2008).

[26] D. J. Wineland, C. Monroe, W. M. Itano, D. Leibfried, B. E. King, and D. M. Meekhof, J.

Res. Natl. Inst. Stand. Technol. **103**, 259 (1998).

[27] A. Steane, Appl.Phys.B **64**, 623 (1997).

[28] F. Schmidt-Kaler, H.Häffner, S. Gulde, M. Riebe, G. P. T. Lancaster, T. Deuschle, C. Becher, W. Hänsel, J. Eschner, C. F. Roos, and R. Blatt, Appl.Phys.B **77**, 789 (2003).

[29] K. J. Blow, R. Loudon, and S. J. D. Phoenix, Phys. Rev. A **42**, 4102 (1990).

[30] M. A. Nielsen and I. L. Chuang, *Quantum Computation and Quantum Information* (Cambridge University Press, 2000).

[31] M. Liang and L. Yang(2010), e-print: quant-ph/1006.4941.

[32] E. Knill, Nature **434**, 39 (2005).

[33] P. Aliferis, D. Gottesman, and J. Preskill, Quantum Inf. Comput. **8**, 181 (2008).

[34] G. J. Milburn, S. Schneider, and D. F. V. James, Fortschr. Phys. **48**, 801 (2000).

[35] D. Leibfried, B. DeMarco, V. Meyer, D. Lucas, M. Barrett, J. Britton, W. M. Itano, B. Jelenković, C. Langer, T. Rosenband, and D. J. Wineland, Nature **422**, 412 (2003).

[36] D. J. Wineland, M. Barrett, J. Britton, J. Chiaverini, B. DeMarco, W. M. Itano, B. Jelenković, C. Langer, D. Leibfried, V. Meyer, T. Rosenband, and T. Schätz, Phil. Trans. R. Soc. **361**, 1349 (2003).

[37] L. Yang and Y. F. Chen(2007), e-print: quant-ph/0712.3197.